

Ethynylene-Linked Oligomers Based on Benzodithiophene: Synthesis and Photoelectric Properties

Songyang Jiang, Yuwen Ma, Yingyi Wang, Chengyun Wang,* and Yongjia Shen

Key Laboratory for Advanced Materials and Institute of Fine Chemicals, East China University of Science and Technology, Shanghai 200237, China

Two conjugated ethynyl-linked oligomers, oligo(benzodithiophene-ethynylene-benzothiadiazole) (O1) and oligo(benzodithiophene-ethynylene-carbazole) (O2), were synthesized by Sonogashira coupling reaction. Their degrees of polymerization were 7 and 10, respectively. Their photophysical and electrochemical properties were investigated. O1 exhibited two strong absorption bands at 404 nm and 483 nm, and O2 at 401 nm and 429 nm. The results of UV-Vis, cyclic voltammetry (CV) and theoretical calculations showed that O1 has a narrower band gap than O2. The conductivities of O1 and O2 were 1.05×10^{-15} and 6.98×10^{-16} S/cm, respectively, and would increase to 1.23×10^{-10} and 1.05×10^{-10} S/cm after doping with iodine.

Keywords benzodithiophene, conjugated polymer, Sonogashira reaction, photoelectric property, conductivity

Introduction

Organic photoelectric materials have recently attracted intense research interest because of their structural diversity. Organic semiconductors consisting of these materials have better flexibility and lower production cost. Moreover, the physical properties (optical behavior, charge carrier mobility, HOMO/LUMO energy levels, and structural ordering) of these organic semiconductors can be tuned by various chemical functionalizations. There are two kinds of charge transports in polymer transistors, namely, interchain transport (π - π stacking orientation) and intrachain transport. The speed of intrachain transport is much faster than that of interchain. Additionally, polymers usually possess good flexibility and thermal stability, which render them the most promising materials for flexible devices with large area.^[1] The rapid development of organic photoelectric materials will definitely make contributions for the global energy crisis.

Polythiophenes, including one-dimensional, two-dimensional and three-dimensional conjugated systems, are one of the largest families of organic semiconductors, which have been used in organic photovoltaic cells (OPVs) due to their high charge-carrier mobility and facile synthesis to tune their energy levels.^[2] Benzo-[1,2-*b*:4,5-*b'*]dithiophene (BDT) has a symmetric and planar conjugated structure, so BDT-based conjugated polymers present a tight and regular stacking, which was widely studied as a photoelectric functional material. BDT unit has been already used as conjugated core

in small molecules and polymers, mostly in OFETs and in OPVs.^[3-10]

BDT was first used in the organic thin film transistor. In 1997, Katz *et al.* reported a new type of p-type organic semiconductor based on benzodithiophene building blocks with expected thermal stability.^[11] Subsequently, Ong *et al.* found that the polymer exhibited excellent field-effect transistor properties with mobility of $0.15 \text{ cm}^2 \cdot \text{V}^{-1} \cdot \text{s}^{-1}$ in thin-film transistor when BDT unit was linked with other electron transport unit. Moreover the preparation of thin-film semiconductor could be processed without thermal annealing.^[8]

In 2007, a polymer based on BDT-thiophene was applied in OFETs with a high field-effect transistor mobility of $0.25 \text{ cm}^2 \cdot \text{V}^{-1} \cdot \text{s}^{-1}$ and current on/off ratio of 10^5 – 10^6 when measured in ambient conditions.^[9] In recent years, the field-effect property was found to be improved by introducing aromatic ethynyl to BDT unit.^[12-14]

Conjugated polymers based on BDT units were first applied in BHJ solar cells by Hou *et al.* at 2008. In their following work, they repeatedly used BDT units as a component for the construction of conjugated polymers, and succeeded in improving the PCE of OPVs beyond 7% in 2010.^[15] And more BDT-containing photoelectric materials were studied and reported,^[16-22] indicating that BDT plays a pivotal role in photovoltaic polymers and other relevant applications.

In this paper, BDT was selected as a donor unit due to its excellent electron donating capability and electron transmitting capability, and benzothiadiazole^[23-29] or

* E-mail: cywang@ecust.edu.cn (C. Y. Wang); Tel.: 0086-021-64252967; Fax: 0086-021-64252967

Received February 12, 2014; accepted March 28, 2014; published online April 22, 2014.

Supporting information for this article is available on the WWW under <http://dx.doi.org/10.1002/cjoc.201400079> or from the author.

carbazole^[30–32] was linked with BDT via acetylene as a bridge to form a D-linker-A conjugated system. By comparison, carbazole showed relatively weaker electron-withdrawing ability than benzothiadiazole. Furthermore, due to the rigidity of acetylene bond, the new oligomers exhibited more reasonable planarity and rigidity, contributing a better π - π stacking effect which would further enhance the electron transmission as a whole. The two novel oligomers were discussed from their optoelectronic property as well as conductivity.

Experimental

Materials

All solvents and reagents, unless otherwise stated, were CP or AR level. Solvents for chemical synthesis such as THF, triethylamine were purified by dehydration and distillation with standard methods. Pd(PPh₃)₂Cl₂ was synthesized according to the reference and stored in dry container.^[33]

Instruments and measurements

¹H NMR and ¹³C NMR data were obtained from a Bruker Avance III 400 (in CDCl₃, TMS as the internal standard). MS data were obtained by Micromass LCTM (HREI-TOF). FT-IR spectra were recorded on a Nicolet Magna-IR 550 spectrometer. The UV-Vis spectra were recorded by a Varian Cary 100 UV-Vis Spectrometer (CHCl₃ as solvent). Fluorescence spectra were recorded by a Varian Cary Eclipse Fluorescence Spectrometer (CHCl₃ as solvent). Cyclic voltammograms were performed with a Versastat II electrochemical workstation. Thermogravimetric analysis (TGA) was carried on a Netzsch STA 409 PC/PG under nitrogen atmosphere. Molecular weights of the polymer were obtained on a Waters 1515 using a calibration curve of polystyrene standards, with tetrahydrofuran as the eluent. The conductivity was measured by PC408 digital insulation resistor tester at room temperature.

Synthesis

Synthesis of 4,8-dioctyloxybenzo[1,2-*b*:4,5-*b'*]-dithiophene (4) Compound **3** (0.96 g, 4.36 mmol) and zinc powder (0.682 g, 10.43 mmol) were suspended in 15 mL of water, then NaOH (2.6 g, 650 mmol) was added into the mixture. The mixture was heated to reflux for 1 h. During the reaction, the color of the mixture changed from yellow to red and then to orange. Subsequently, 1-bromooctane (2.53 g, 13.12 mmol) and TBAB (0.28 g, 0.87 mmol) were added into the flask. After being refluxed for 12 h, the reactant was poured into 70 mL cold water and extracted by 100 mL of methylene chloride for three times. The organic layer was dried by anhydrous Na₂SO₄. After removing solvent, the crude product was purified by column chromatography (methylene chloride : petroleum ether = 1 : 15), compound **4** (1.45 g, 3.25 mmol, yield 74.3%) was obtained as white crystal. m.p. 46.0–47.1 °C; ¹H NMR (400

MHz, CDCl₃) δ : 7.48 (d, J =5.6 Hz, 2H, thienyl H), 7.37 (d, J =5.6 Hz, 2H, thienyl H), 4.27 (t, J =6.8 Hz, 4H, OCH₂), 1.87 (q, J =6.8 Hz, 4H, CH₂), 1.53–1.58 (m, 4H, CH₂), 1.38–1.25 [m, 16H, (CH₂)₄], 0.88 (t, J =7.2 Hz, 6H, CH₃).

Synthesis of 2,6-dibromo-4,8-dioctyloxybenzo[1,2-*b*:4,5-*b'*]-dithiophene (5) Compound **4** (1.02 g, 2.28 mmol) was dissolved into 30 mL of methylene chloride in a 100 mL three-neck flask. Bromine (0.764 g, 4.78 mmol) was dissolved into 20 mL of methylene chloride in a funnel and slowly dropped into the flask under an ice-water bath, and then the mixture was stirred for 7 h at room temperature. After removing solvent, the crude product was purified by column chromatography (methylene chloride : petroleum ether = 1 : 7), compound **5** (1.238 g, 2.048 mmol, yield 93.65%) was obtained as white solid. m.p. 58.3–59.3 °C; ¹H NMR (400 MHz, CDCl₃) δ : 7.42 (s, 2H, thienyl H), 4.19 (t, J =6.8 Hz, 4H, OCH₂), 1.83 (quintuple, J =6.8 Hz, 4H, CH₂), 1.49–1.55 (m, 4H, CH₂), 1.37–1.30 [m, 16H, (CH₂)₄], 0.90 (t, J =6.8 Hz, 6H, CH₃); ¹³C NMR (100 MHz, CDCl₃) δ : 142.3, 131.2, 130.9, 123.2, 115.0, 74.2, 31.8, 30.4, 29.4, 29.3, 26.0, 22.7, 14.1; HRMS (ESI) m/z : [M+H]⁺ calcd for C₂₆H₃₇Br₂O₂S₂ 603.0602, found 603.0604.

Synthesis of 2,6-trimethylsilyl-4,8-dioctyloxybenzo[1,2-*b*:4,5-*b'*]-dithiophene (6) Compound **5** (1.01 g, 1.67 mmol) was dissolved into 30 mL THF and 20 mL triethylamine in a 100 mL three-neck flask, degassed with Ar over 30 min. Then, Pd(PPh₃)₂Cl₂ (58.5 mg, 0.08 mmol) and CuI (31.8 mg, 0.167 mmol) were added into the flask under Ar atmosphere. Subsequently, trimethylsilylacetylene (1.31 g, 13.34 mmol) was added dropwise under Ar atmosphere. The mixture was stirred at room temperature for 7 h. After removing solvent, the crude product was purified by column chromatography (methylene chloride : petroleum ether = 1 : 15), compound **6** (0.962 g, 1.505 mmol, yield 90.18%) was obtained as yellow solid. m.p. 99.6–101.2 °C; ¹H NMR (400 MHz, CDCl₃) δ : 7.56 (s, 2H, thienyl H), 4.21 (t, J =6.8 Hz, 4H, OCH₂), 1.84 (quintuple, J =6.8 Hz, 4H, CH₂), 1.51–1.54 (m, 4H, CH₂), 1.37–1.30 [m, 16H, (CH₂)₄], 0.90 (t, J =6.8 Hz, 6H, CH₃), 0.28 (s, 18H, SiCH₃); ¹³C NMR (100 MHz, CDCl₃) δ : 144.1, 132.0, 130.4, 126.2, 123.1, 101.9, 98.0, 74.4, 32.0, 30.7, 29.6, 29.5, 26.2, 22.9, 14.4, 0.22; HRMS (ESI) m/z : [M+H]⁺ calcd for C₃₆H₅₅O₂S₂Si₂ 639.3182, found 639.3177.

Synthesis of 2,6-bisacetynyl-4,8-dioctyloxybenzo[1,2-*b*:4,5-*b'*]-dithiophene (7) Compound **6** (0.855 g, 1.338 mmol) was dissolved into 20 mL THF in a 50 mL flask, then TBAF (1.267 g, 4 mmol) was added into the flask. The mixture was stirred for 40 min. Subsequently, the solvent was removed and the crude product was purified by column chromatography (methylene chloride : petroleum ether = 1 : 7), compound **7** (0.637 g, 1.288 mmol, yield 96.24%) was obtained as claybank solid. m.p. 66.2–67.8 °C; ¹H NMR (400 MHz, CDCl₃) δ : 7.62 (s, 2H, thienyl H), 4.23 (t, J =6.8 Hz, 4H,

OCH₂), 3.48 (s, 2H, alkynyl H), 1.85 (quintuple, $J=6.8$ Hz, 4H, CH₂), 1.50–1.55 (m, 4H, CH₂), 1.36–1.30 [m, 16H, (CH₂)₄], 0.90 (t, $J=6.8$ Hz, 6H, CH₃); ¹³C NMR (100 MHz, CDCl₃) δ : 144.0, 131.7, 130.2, 126.6, 121.9, 100.6, 83.5, 74.2, 31.8, 30.5, 29.4, 29.2, 26.0, 22.7, 14.1; HRMS (ESI) m/z : [M + H]⁺ calcd for C₃₀H₃₉O₂S₂ 495.2391, found 495.2390.

Synthesis of benzothiadiazole (8) *O*-Phenylenediamine (3.25 g, 0.03 mol) was dissolved into 60 mL methylene chloride and 18 mL triethylamine in a 250 mL three-neck flask, then SOCl₂ (7 mL, 0.096 mol) was added dropwise in 1 h through a funnel. Kept the mixture refluxing for 16 h, then 30 mL water and 80 mL 1 mol/L NaOH aqueous solution were successively added when the reactant cooled to room temperature. The mixture was extracted by 100 mL of methylene chloride for three times. The organic layer was dried by anhydrous Na₂SO₄. After removing solvent, compound **8** (3.326 g, 24.43 mmol, yield 81.3%) was obtained as red brown crystal. ¹H NMR (400 MHz, CDCl₃) δ : 8.04–8.00 (m, 2H, ArH), 7.62–7.57 (m, 2H, ArH).

Synthesis of 3,6-dibromobenzothiadiazole (9) Compound **8** (1.36 g, 0.01 mol) was dissolved into 35 mL 40% HBr aqueous solution in a 250 mL three-neck flask. Then 30 mL 40% HBr and 1.6 mL Br₂ were added dropwise from a funnel. Subsequently, another 20 mL 40% HBr was added again from funnel. Kept the reactant refluxing for 12 h, and then cooled to room temperature. The reaction mixture was poured into excess saturated NaHSO₃ aqueous solution. Then the mixture was filtrated, and the yellowish white solid was washed by 30 mL of water thrice and 20 mL diethyl ether thrice. The crude product was purified by recrystallization from ethyl alcohol. Compound **9** (1.901 g, 6.47 mmol, yield 64.27%) was obtained as a yellowish white powder. m.p. 187.2–187.3 °C; ¹H NMR (400 MHz, CDCl₃) δ : 7.74 (s, 2H, ArH); ¹³C NMR (100 MHz, CDCl₃) δ : 132.4, 122.7, 113.9.

Synthesis of 3,6-diiodocarbazole (10) Carbazole (3 g, 17.94 mmol), KI (3.9 g, 23.5 mmol) and KIO₃ (5.1 g, 23.5 mmol) were dissolved into 75 mL HAc in a 250 mL three-neck flask, and the temperature of the mixture was maintained at 80 °C for 6 h. After cooling to room temperature, the mixture was filtrated, and the crude product was washed successively by water, saturate Na₂CO₃, saturate Na₂S₂O₃ and water. The crude product was purified by recrystallization from ethyl alcohol. compound **10** (5.0 g, 11.93 mmol, yield 66.52%) was obtained as a white solid. m.p. 204.5.5–204.7 °C; ¹H NMR (400 MHz, CDCl₃) δ : 8.33 (d, $J=1.6$ Hz, 2H, ArH), 8.07 (s, 1H, NH), 7.68 (dd, $J_1=1.6$ Hz, $J_2=8.8$ Hz, 2H, ArH), 7.22 (d, $J=8.8$ Hz, 2H, ArH).

Synthesis of *N*-octyl-3,6-diiodocarbazole (11) Compound **10** (2.1 g, 5 mmol) was dissolved into 20 mL DMF in a 100 mL three-neck flask, 1-bromooctane (1.16 g, 6 mmol) and K₂CO₃ (3.5 g, 25 mmol) were added in the flask. Then the mixture was maintained at 80 °C for 4 h under Ar atmosphere. After cooling to

room temperature, the cold reaction mixture was poured into 100 mL water. Subsequently, the mixture was filtered, and filter cake was washed by water. The crude product was purified by recrystallization from *n*-hexane. Compound **11** (2.12 g, 3.98 mmol, yield 80%) was acquired as a earthy yellow powder. m.p. 97.0–98.1 °C; ¹H NMR (400 MHz, CDCl₃) δ : 8.33 (s, 2H, ArH), 7.71 (d, $J=8.8$ Hz, 2H, NH), 7.18 (dd, $J_1=1.6$ Hz, $J_2=8.8$ Hz, 2H, ArH), 4.22 (t, $J=7.2$ Hz, 2H, NCH₂), 1.83–1.78 (m, 2H, CH₂), 1.30–1.22 (m, 10H, CH₂), 0.86 (t, $J=6.8$ Hz, 3H, CH₃); ¹³C NMR (100 MHz, CDCl₃) δ : 139.5, 134.5, 129.4, 124.0, 110.9, 81.6, 43.3, 31.8, 29.3, 29.1, 28.8, 27.2, 22.6, 14.1; HRMS (ESI) m/z : [M + H]⁺ calcd for C₂₀H₂₄I₂N 531.9998, found, 531.9996.

Synthesis of oligo(2,6-bisacetenyl-4,8-dioctyloxybenzo[1,2-*b*:4,5-*b'*]dithiophene-alt-3,6-dibromobenzothiadiazole) (O1) Compound **7** (123.7 mg, 0.25 mmol) and compound **9** (73.5 mg, 0.25 mmol) were dissolved in the mixture of tetrahydrofuran (8 mL) and Et₃N (5 mL) in a 50 mL three-neck flask, then degassed with Ar over 30 min. Then, Pd(PPh₃)₄ (30 mg) and CuI (10 mg) were added into the flask under Ar atmosphere. The mixture was stirred at room temperature for 12 h. Subsequently, the mixture was filtered and the solvent was removed. The residue was dissolved in 3 mL CHCl₃, and precipitated with adding 35 mL methanol. The procedure was repeated 3 times to remove unreacted monomers and low molecular weight oligomers. After this procedure, the precipitation was collected by vacuum filtration and dried in vacuum for 3 h at 60 °C. The oligomer **O1** (100 mg, 50.76%) was obtained as red brown powder. λ_{\max} : 404, 483 nm; ¹H NMR (400 MHz, CDCl₃) δ : 7.88–7.45 (m, 4H, ArH), 4.30–4.18 (m, 4H, OCH₂), 2.01–1.89 (m, 4H, CH₂), 1.40–1.25 (m, 20H, CH₂), 0.90 (t, $J=6.8$ Hz, 6H, CH₃); IR (KBr) ν : 3410, 2147, 1637, 879 cm⁻¹.

Synthesis of oligo(2,6-bisacetenyl-4,8-dioctyloxybenzo[1,2-*b*:4,5-*b'*]dithiophene-alt-*N*-octyl-3,6-diiodocarbazole) (O2) **O2** (0.147 g, 70.91%) was prepared similarly to **O1**. λ_{\max} : 401, 429 nm; ¹H NMR (400 MHz, CDCl₃) δ : 8.40–7.16 (m, 8H, ArH), 4.30–4.27 (m, 6H, OCH₂ and NCH₂), 1.89–1.87 (m, 6H, CH₂), 1.40–1.25 (m, 30H, CH₂), 0.92–0.85 (m, 9H, CH₃); IR (KBr) ν : 3410, 2135, 1286, 1261, 1033 cm⁻¹.

All the spectra of ¹H NMR, ¹³C NMR and other relevant data were list in Supporting Information.

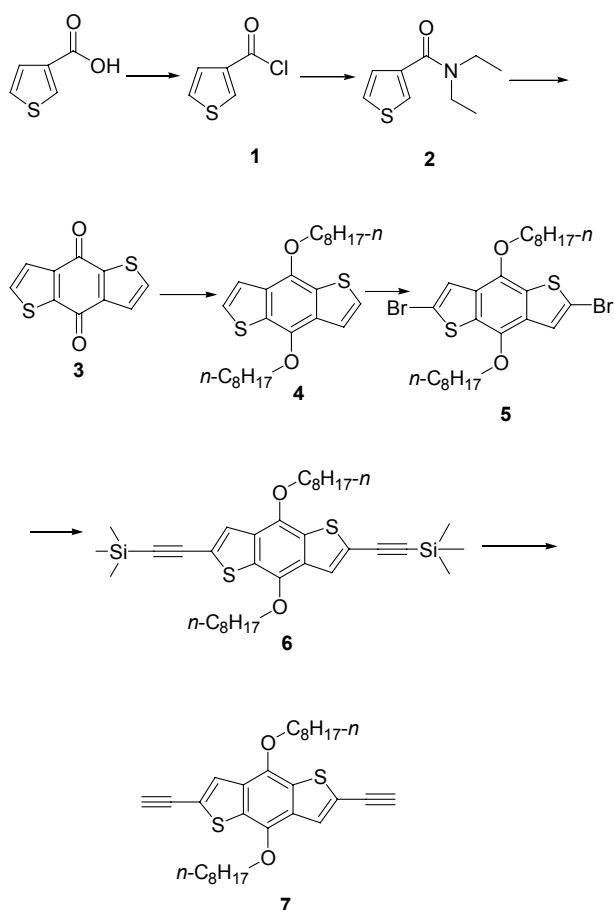
Results and Discussion

Synthesis and characterization

Synthesis Scheme 1 illustrates the general synthetic routes toward the BDT monomer **7**. Compounds **1–3** were prepared according to the literature.^[8,34] Compound **4** was synthesized by a reduction reaction and a substitution reaction. Compound **3** was firstly reduced by Zn powder in NaOH aqueous solution, and then the substitution reaction occurred after 1-bromododecane was added into the mixture. Compound **4** was

brominated via Br_2 to prepare compound **5** at low temperature. Then compound **6** was synthesized by Sonogashira coupling reaction in mixed solvents of THF and TEA. This step occurred under Argon and dry conditions, utilizing $\text{Pd}(\text{PPh}_3)_2\text{Cl}_2/\text{CuI}$ as catalyst. The trimethylsilyl of compound **6** was removed by TBAF to obtain monomer **7**.

Scheme 1 Synthesis of 2,6-bisacetynyl-4,8-dioctyloxybenzo[1,2-*b*:4,5-*b'*]dithiophene



As shown in Scheme 1, Zn powder (about 1.2 equiv.) was used excessively to ensure that the quinoid structure was fully reduced for the preparation of compound **4**. Then $n\text{-C}_8\text{H}_{17}\text{Br}$ (1.5 equiv.) was added into the mixture. The reaction needed to be sustained for 12 h, otherwise the substitution reaction could not proceed completely. This factor will affect the yield, and the yield of this step is up to 74.3%, which is higher than those in similar literatures.^[18,35]

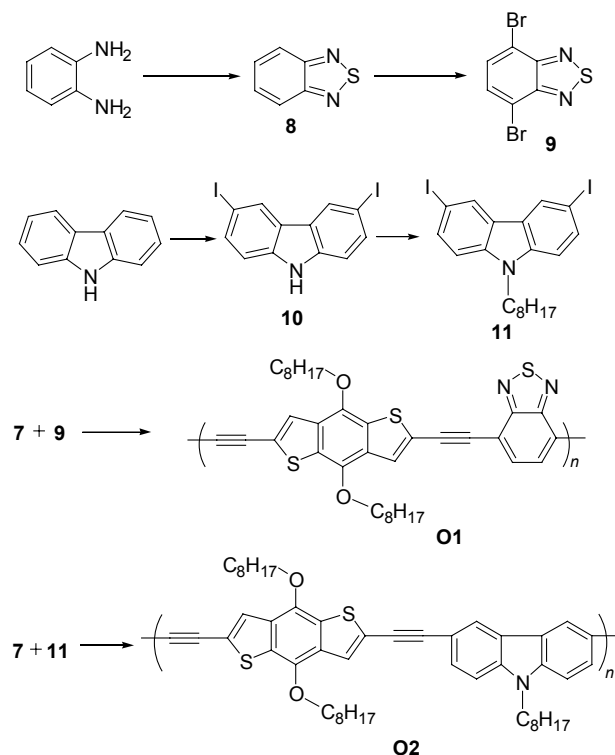
In the transformation from compound **4** to compound **5**, 4,8-substituted BDT (**4**) has two pairs of protons, and the chemical behaviors of these protons are similar as the protons on a thiophene unit. The protons on 2 and 6 positions exhibit lower $\text{p}K_{\text{a}}$ value than the protons on 3 and 7 positions,^[3] so the protons on 2 and 6 positions are more reactive. However, we must strictly control the amount of liquid bromine (1 equiv.), and the temperature should be lower than room temperature. We conduct this reaction under ice-water bath, and the reac-

tion time was determined by TLC test. The yield is up to 93.65%, higher than that of literature.^[9]

The synthetic methods of compound **7** were summarized as follows. At first, we used KOH and K_2CO_3 as base, MeOH/DCM or isopropanol as solvent,^[36] but the result was not satisfactory. Due to worse solubility of base, the reaction was unsuccessful, especially when MeOH and DCM were used as reaction solvents. Therefore, we used tetrabutylammonium fluoride (TBAF) acting as base and THF as solvent. Then the base dissolved well and the reaction rate was fast. The best reaction molar ratio of compound **6** vs. TBAF was 1 : 3, and the reaction time was approximately 30 min. This phenomenon may be ascribed to the strong combining capacity of fluorine atom and silicon atom, demonstrating that TBAF is a good choice to remove trimethylsilyl.

Scheme 2 illustrates the general synthetic routes of monomer **9**, monomer **11**, **O1** and **O2**. Monomer **9** and monomer **11** were synthesized according to previous literature.^[37,38]

Scheme 2 Synthesis of monomer **9**, monomer **11**, **O1** and **O2**



O1 and **O2** were synthesized by a Palladium-catalyzed Sonogashira coupling reaction. The reaction condition and purification process were almost under the same condition besides the reaction time of **O2** was 3 d, **O1** just 12 h. All of them were proceeded under argon and dry environment in mixed solvents of THF and Et_3N , catalyzed by $\text{Pd}(\text{PPh}_3)_2\text{Cl}_2$ and CuI . The oligomers were precipitated from $\text{CH}_3\text{OH}/\text{CHCl}_3$ for three times in order to remove small molecules.

Characterization The oligomers were character-

ized by ^1H NMR (Figure 1 and Figure 2) and FT-IR spectroscopy. ^1H NMR spectrum indicated the chemical structure of each monomer unit of the alternating oligomers, and the results confirmed their chemical structures. Characteristic proton resonances for **O1** were assigned as follows: resonance at δ 7.88–7.45 for Ar-H, resonance at δ 4.30–4.18 for methylene H located near oxygen atom, and resonance at δ 1.40–1.25 for methyl H. **O2** can be characterized by ^1H NMR in the same way. (see the Experimental Section for details).

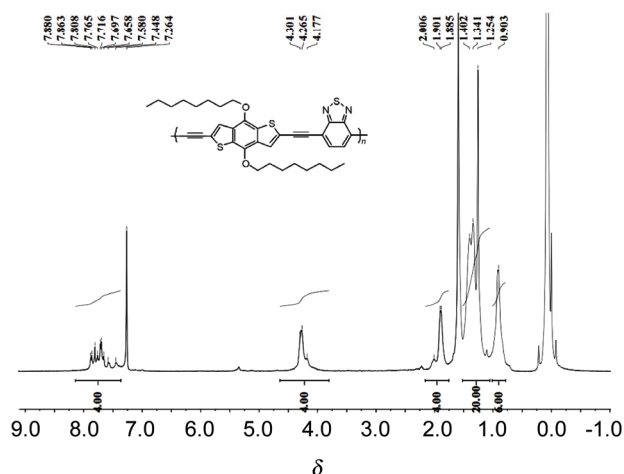


Figure 1 ^1H NMR spectrum of **O1**.

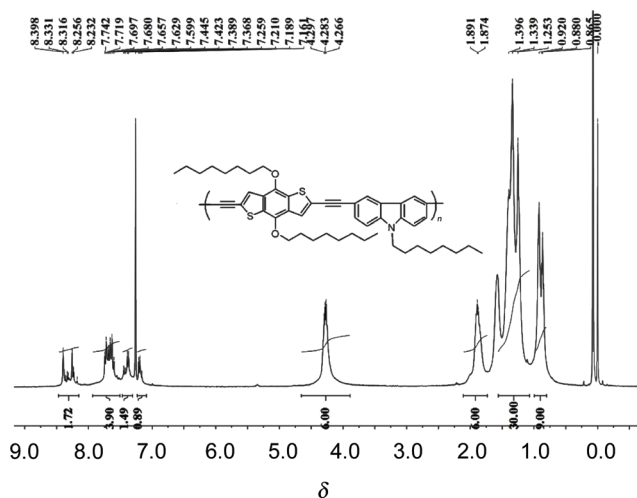


Figure 2 ^1H NMR spectrum of **O2**.

The FT-IR spectra of **O1** and **O2** are shown in Figure 3. For **O1**, we can find a $\equiv\text{C}-\text{H}$ stretching vibration at 3409 cm^{-1} and $\text{C}\equiv\text{C}$ stretching vibration at 2147 cm^{-1} , $\text{C}=\text{N}$ stretching vibration at 1637 cm^{-1} , $\text{C}-\text{Br}$ stretching vibration at 879.42 cm^{-1} . For **O2**, its FT-IR spectrum is similar to that of **O1**, $\text{N}-\text{C}$ stretching vibration at 1286.25 cm^{-1} , $\equiv\text{C}-\text{O}-\text{C}$ stretching vibration at 1261.28 and 1033.71 cm^{-1} .

The molecular weight was measured by GPC using polystyrene as the standard, with THF as the eluent, and corresponding data were summarized in Table 1. The number-average molecular weight (M_n) is 4502 Da for **O1** and 7369 Da for **O2**, respectively. Corresponding

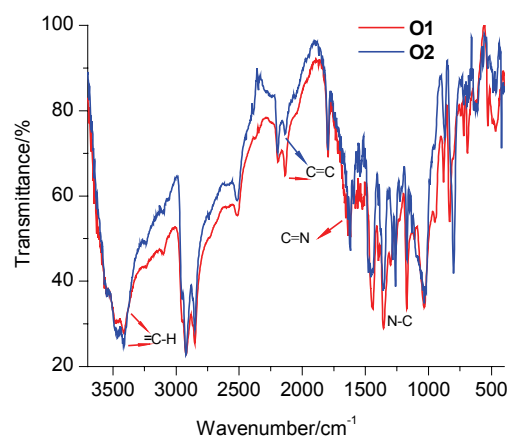


Figure 3 FT-IR spectra of **O1** and **O2**.

Table 1 Molecular weights and thermal properties of **O1** and **O2**

| Oligomer | M_n/Da | M_w/Da | PDI | n | $T_d/^\circ\text{C}$ |
|-----------|-----------------|-----------------|------|-----|----------------------|
| O1 | 4502 | 5079 | 1.13 | 7 | 285 |
| O2 | 7369 | 7658 | 1.04 | 10 | 326 |

degrees of polymerization (n) are 7 and 10, and their PDI are 1.13 and 1.04, respectively. The low value of n may be attributed to steric hindrance and solubility of polymers. **O1** has a worse solubility in organic solvent than **O2**, because **O2** has more octyl groups. More alkyl chains were introduced into the system, which can enhance their solubility. However, more octyl groups will hinder the rotation of conjugated structure. These factors will hamper the polymerization.

UV-Vis absorption and fluorescence emission spectra

The UV-Vis absorption spectra and fluorescence emission spectra of **O1** and **O2** in CHCl_3 solutions are shown in Figure 4 and Table 2, respectively. The absorption spectrum of **O1** showed two major peaks located at 404 and 483 nm, and **O2** also showed two major peaks located at 401 and 429 nm.

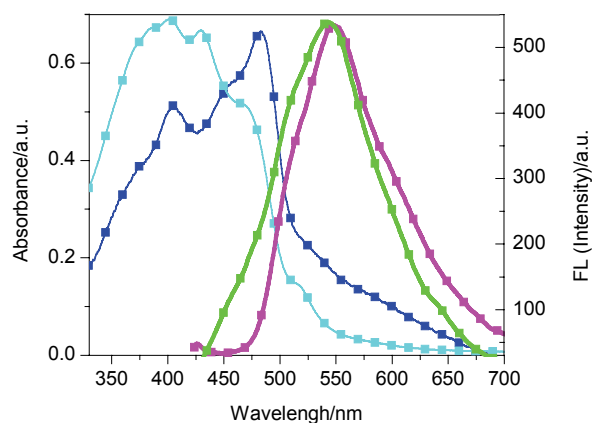


Figure 4 UV-Vis absorption spectra of **O1** (blue line) and **O2** (red line) and fluorescence emission spectra of **O1** (violet) and **O2** (green) in CHCl_3 solutions.

Both the oligomers exhibited an absorption band at approximately 400 nm to 500 nm arising from π - π^* transitions of the large conjugated system. However, **O1** showed a strong absorption with λ_{max} at 483 nm, which is 54 nm red shifted from those of **O2** (λ_{max} at 429 nm). It reveals that the light with lower energy or larger wavelength could be absorbed by **O1**. This phenomenon may be ascribed to the difference of their structures. Benzothiadiazole is probably a group with stronger electron-withdrawing ability than carbazole. In general, D- π -A system has a lower band gap than normal system, because the intramolecular charge transfer effect exists in the D- π -A system, which is helpful for the transportation of electron.

Table 2 Photophysical properties of **O1** and **O2**

| Oligomer | Absorption peak λ_{max} /nm | E_g /eV | Excitation wavelength/nm | Maximum emission λ_{max} /nm |
|-----------|--|-----------|--------------------------|---|
| O1 | 404, 483 | 1.92 | 404 | 550 |
| O2 | 401, 429 | 2.27 | 401 | 545 |

The optical band gaps estimated from the onsets of their absorption spectra were according to the literature,^[39] and the $h\nu$ - $(\alpha h\nu)^2$ dependences of **O1** and **O2** were shown in Figure 5. The results showed that their optical band gaps were 1.92 and 2.27 eV, respectively. For the construction of small band gap polymers, many examples^[40,41] have demonstrated that utilizing alternative electron deficient and electron rich units is an effective method. The difference of optical band gap is particularly owed to the different molecular structures and the number of electron donating functional groups.^[42,43] Both of them have relatively small band gap, so the electron transition is easy to occur. It is suitable for the applications in photoelectric materials, especially for **O1**. The ideal band gap of photoelectric materials is below 2 eV.^[44]

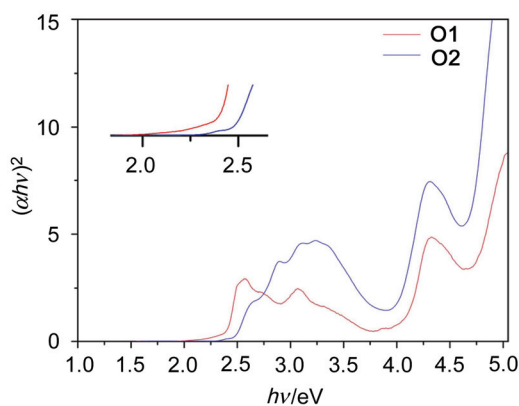


Figure 5 The calculated curve of optical band gap of **O1** and **O2** ($h=6.626 \times 10^{-34}$ J·s; $\nu=1/\lambda$; α =absorbance).

The fluorescence emission spectra of **O1** and **O2** in CHCl_3 at room temperature are also shown in Figure 4.

The fluorescence emission spectra showed a broad emission band over 450–680 nm, and the maximum emission peak of **O1** is located at 550 nm, approximate to the peak of **O2** at 545 nm. The two oligomer's Stokes shift is approximate to 145 nm.

Thermal properties

The thermal properties of the target oligomers were obtained by thermogravimetric analysis (TGA) under nitrogen. Table 1 summarizes the results and their TGA thermograms are given in Figure 6. The TGA curves showed that the oligomers were thermally stable with an initial decomposition temperature in a N_2 atmosphere at 128 °C for **O1** and 252 °C for **O2**, and 5% weight loss (T_5) of 285 °C for **O1** and 326 °C for **O2**, respectively. When weight loss was over 30%, **O2** was more thermally stable than **O1** due to the better stability of carbazole than BDT unit.

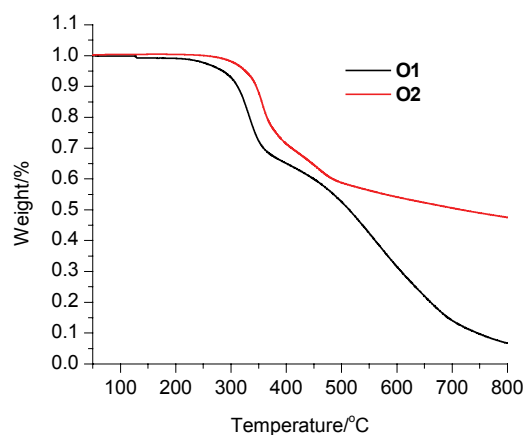


Figure 6 TGA curves of **O1** and **O2** at a heating rate of 10 °C/min under N_2 atmosphere.

Cyclic voltammetry (CV)

The electrochemical behavior of the oligomers was investigated by cyclic voltammetry (CV), as shown in Figure 7. The oligomer powder was dissolved in an electrolyte solution of 0.1 mol/L tetrabutylammonium hexafluorophosphate (TBAPF₆) in CHCl_3 . In the measurement, we used Pt as working electrode, saturated calomel electrode (SCE) as reference electrode and glassy carbon electrode as counter electrode at room temperature. Cyclic voltammeteries (CVs) performed in the whole potential range between 0 and 1.5 V showed several redox processes.

The highest occupied molecular orbital (HOMO) levels and the lowest unoccupied molecular orbital (LUMO) levels were calculated by CV curve and λ_{onset} . The result was shown in Table 3. The HOMO levels of **O1** and **O2** are -5.64 and -5.66 eV, and the LUMO of **O1** and **O2** are -3.72 and -3.39 eV, respectively. Both of them have a relatively deep HOMO energy level which implies that these oligomers have good stability in the air. These oligomers maybe have potential

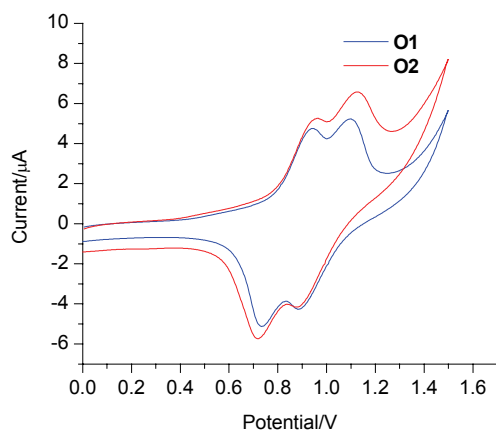


Figure 7 CV of **O1** and **O2** in 0.1 mol/L TBAPF₆·CHCl₃ solution at 20 mV/s.

applications in organic photoelectric and photovoltaic materials due to the relatively low HOMO energy level.^[45]

Table 3 Electrochemical properties and band gap of **O1** and **O2**

| Oligomer | $E_{\text{onset-ox}}^a/\text{V}$ | HOMO ^b /eV | E_g^c/eV | LUMO ^d /eV |
|-----------|----------------------------------|-----------------------|-------------------|-----------------------|
| O1 | 0.94 | -5.64 | 1.92 | -3.72 |
| O2 | 0.96 | -5.66 | 2.27 | -3.39 |

^a $E_{\text{onset-ox}}$ = onset oxidation potential measured by cyclic voltammetry. ^b HOMO = $-e(E_{\text{onset-ox}} + 4.7)$ (eV). ^c E_g estimated from the UV-Vis absorption spectra. ^d LUMO = $E_g + \text{HOMO}$.

Density functional theoretical calculations

Density functional theory (DFT) calculations were performed at B3LYP/6-31G* level using dimer models, benzodithiophene-ethynylene-benzothiadiazole and benzodithiophene-ethynylene-carbazole. The optimized geometries and electron distributions of **O1** and **O2** were calculated by DFT method with B3LYP/6-31G (d) basis sets using Gaussian 03 code. In order to calculate conveniently, we used oligomers' dimer models, benzodithiophene-ethynylene-benzothiadiazole and benzodithiophene-ethynylene-carbazole, to replace **O1** and **O2**. The results were shown in Figure 8 and Table 4. The HOMO of **O1** was mainly delocalized through BDT unit and acetylene bond, and the LUMO of **O1** was populated over benzothiadiazole and acetylene bond. This phenomenon is an ideal condition for photoelectric materials. The benzothiadiazole group plays an acceptor role to BDT unit, which is beneficial to intramolecular electron migration. It can be concluded that **O1** will have a good conductivity. The calculated HOMO level of **O1** is -5.3 eV and the LUMO level is -2.6 eV.

The HOMO of **O2** is distributed almost overall conjugated backbone, and the LUMO of **O2** is also populated over entire conjugated backbone. This phenomenon can be attributed to the similar electron-withdrawing ability of BDT and Carbazole. Compared with HOMO state, the electron clouds in LUMO state slightly flow to BDT unit. The calculated HOMO level

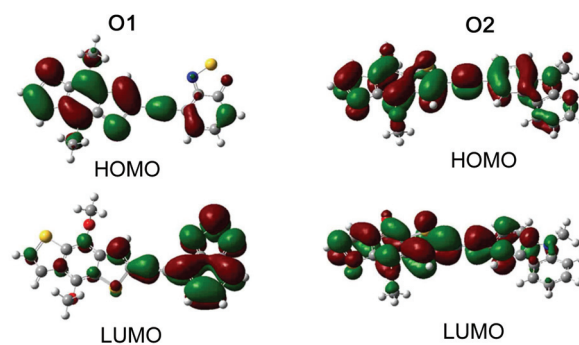


Figure 8 Frontier molecular orbital profiles of **O1** and **O2**.

Table 4 The calculated energy levels of oligomers by B3LYP/6-31G

| Oligomer | HOMO/eV | LUMO/eV | E_g/eV |
|-----------|---------|---------|-----------------|
| O1 | -5.3 | -2.6 | 2.7 |
| O2 | -5.0 | -1.5 | 3.5 |

of **O2** is -5.0 eV and the LUMO level is -1.5 eV. Obviously, **O1** has a narrow band gap than **O2**, it is due to the different electron-withdrawing abilities of benzothiadiazole and carbazole.

The calculated band gaps are obviously greater than those estimated by absorption onset values. The results are mainly caused by the difference of dimer models used in the DFT calculations and the realistic oligomers. The dimer models are little molecules, while **O1** and **O2** have degrees of polymerization for 7 and 10, respectively.

Electrical conductivity

Materials preparation: The solutions of **O1** and **O2** in CHCl₃ were treated with iodine by various proportions, and the CHCl₃ was volatilized at room temperature. Then the residue was dried at 30 °C for 5 h. The conductivity was measured by PC408 digital insulation resistor tester at room temperature. The thin film used for testing is prepared through tablet press under a pressure of 20 MPa, which had a diameter about 12 mm.

Electrical conductivity: The results were shown in Table 5. Pure **O1** occupied a poor conductivity approximate to $1.0 \times 10^{-15} \text{ S}\cdot\text{cm}^{-1}$, and the conductivity of **O1** increased to 4.37×10^{-12} and 1.23×10^{-10} with the ratio of doped iodine at 10% and 30%, respectively. Pure **O2** was close to $7 \times 10^{-16} \text{ S}\cdot\text{cm}^{-1}$, and the conductivity of **O2** increased to 1.33×10^{-12} and 1.05×10^{-10} with the ratio of doped iodine at 10% and 30%, respectively. The conductivity of oligomers was increased by 5–6 order of magnitudes. **O1** has a larger conductivity than **O2** because of the difference in their oligomers molecular structure. The benzothiadiazole has a stronger electron-withdrawing ability than carbazole unit. The electron transmission in **O1** is better than **O2**, due to the better ICT (intramolecular charge transfer) effect and better π - π^* stacking effect in **O1** than **O2** which has

more octyl groups in carbazole unit. The data verified the results from theoretical calculations as illustrated in Table 4 and Figure 8.

Table 5 The conductivity of initial oligomer and those doped with iodine

| Oligomer | Ratio of iodine ^a | Conductivity $\sigma/(S \cdot cm^{-1})$ | Oligomer | Ratio of iodine | Conductivity $\sigma/(S \cdot cm^{-1})$ |
|-----------|------------------------------|---|-----------|-----------------|---|
| O1 | 0% | 1.05×10^{-15} | O2 | 0% | 6.98×10^{-16} |
| O1 | 10% | 4.37×10^{-12} | O2 | 10% | 1.33×10^{-12} |
| O1 | 30% | 1.23×10^{-10} | O2 | 30% | 1.05×10^{-10} |

^a Ratio of iodine—the quality percentage of iodine in oligomers.

When polymer was exposed to iodine, the polymer was oxidized by iodine and electron was moved out from polymer. Then the polymer was translated into cation radical, which was so instable that it would capture another electron from adjacent unsaturated bond, generating new cation radical. As the process repeated, the electron could transfer along the conjugated chain.^[46] For **O1** and **O2**, an electron was captured from large conjugated system by iodine, then the electron hole was stuffed by adjacent electron, thereby the electron flowed along conjugated chain (BDT unit and benzothiadiazole or carbazole). When the iodine was doped into **O1** and **O2**, the conductivity of oligomers acquired enormous changes. The electrical behavior of oligomers showed translation from insulator to semi-conductor after the addition of iodine. The conductivity increased obviously with the addition of iodine.

Conclusions

Two novel organic conjugated oligomers, **O1** and **O2**, were successfully synthesized by Pd(II)-catalyzed Sonogashira coupling reaction. **O2** was very soluble in normal organic solvents due to containing octyl group. The degree of polymerization of **O1** is 7, and that of **O2** is 10. Both of them have a good PDI. **O2** was more thermally stable than **O1**. UV-Vis, CV and theoretical calculations show that **O1** had a lower band gap than **O2**, and **O1** had a strong absorption peak which was 54 nm red shifted to **O2**. This phenomenon may be ascribed to the difference of their molecular structures. The stocks shift is about 145 nm for both **O1** and **O2**. From the results of electrical conductivity, **O1** and **O2** showed semi-conductor behavior when doped with iodine, which makes these oligomers have potential applications in organic photoelectric materials.

Acknowledgement

The authors are grateful to financial support from the National Natural Science Foundation of China (Nos. 20872035, 21076078), and the East China University of Science and Technology.

References

- [1] Wang, C.; Dong, H.; Hu, W.; Liu, Y.; Zhu, D. *Chem. Rev.* **2012**, *112*, 2208.
- [2] Zhang, F.; Wu, D.; Xu, Y.; Feng, X. *J. Mater. Chem.* **2011**, *21*, 17590.
- [3] Huo, L.; Hou, J. *Polym. Chem.* **2011**, *2*, 2453.
- [4] Katz, H. E.; Bao, Z.; Gilat, S. L. *Acc. Chem. Res.* **2001**, *34*, 359.
- [5] Takimiya, K.; Kunugi, Y.; Otsubo, T. *Chem. Lett.* **2007**, *36*, 578.
- [6] Kashiki, T.; Miyazaki, E.; Takimiya, K. *Chem. Lett.* **2008**, *37*, 284.
- [7] Pan, H.; Li, Y.; Wu, Y.; Liu, P.; Ong, B. S.; Zhu, S.; Xu, G. *Chem. Mater.* **2006**, *18*, 3237.
- [8] Pan, H.; Wu, Y.; Li, Y.; Liu, P.; Ong, B. S.; Zhu, S.; Xu, G. *Adv. Funct. Mater.* **2007**, *17*, 3574.
- [9] Pan, H.; Li, Y.; Wu, Y.; Liu, P.; Ong, B. S.; Zhu, S.; Xu, G. *J. Am. Chem. Soc.* **2007**, *129*, 4112.
- [10] Chen, L.; Shen, X.; Chen, Y. *Chin. J. Chem.* **2012**, *30*, 2219.
- [11] Laquindanum, J. G.; Katz, H. E.; Lovinger, A. J.; Dodabalapur, A. *Adv. Mater.* **1997**, *9*, 36.
- [12] Leenen, M. A. M.; Cucinotta, F.; Viani, L.; Mavrinskiy, A.; Pisula, W.; Gierschner, J.; Cornil, J.; Schwab, A. P.; Thiem, H.; Müllen, K.; Cola, L. C. *J. Phys. Chem. B* **2010**, *114*, 14614.
- [13] Meng, Q.; Jiang, L.; Wei, Z.; Wang, C.; Zhao, H.; Li, H.; Xu, W.; Hu, W. *J. Mater. Chem.* **2012**, *20*, 10931.
- [14] Sista, P.; Bhatt, M. P.; Mccary, A. R.; Nguyen, H.; Hao, J.; Biewer, M. C.; Stefan, M. C. *J. Polym. Sci., Part A: Polym. Chem.* **2011**, *49*, 2292.
- [15] Hou, J.; Park, M. H.; Zhang, S.; Yao, Y.; Chen, L. M.; Li, J. H.; Yang, Y. *Macromolecules* **2008**, *41*, 6012.
- [16] Braunecker, W. A.; Oosterhout, S. D.; Owczarczyk, Z. R.; Larsen, R. E.; Larson, B. W.; Ginley, D. S.; Boltalina, O. V.; Strauss, S. H.; Kopidakis, N.; Olson, D. C. *Macromolecules* **2013**, *46*, 3367.
- [17] Huo, L.; Zhang, S.; Guo, X.; Xu, F.; Li, Y.; Hou, J. *Angew. Chem., Int. Ed.* **2011**, *50*, 9697.
- [18] Shen, P.; Bin, H.; Chen, X.; Li, Y. *Org. Electron.* **2013**, *14*, 3152.
- [19] Hou, J.; Chen, H. Y.; Zhang, S.; Chen, R. I.; Yang, Y.; Wu, Y.; Li, G. *J. Am. Chem. Soc.* **2009**, *131*, 15586.
- [20] Piliago, C.; Holcombe, T. W.; Douglas, J. D.; Woo, C. H.; BeauJuge, P. M.; Fréchet, J. M. J. *J. Am. Chem. Soc.* **2010**, *132*, 7595.
- [21] Price, S. C.; Stuart, A. C.; Yang, L.; Zhou, H.; You, W. *J. Am. Chem. Soc.* **2011**, *133*, 4625.
- [22] Hu, C.; Zhang, Q. *Chin. J. Chem.* **2013**, *31*, 1404.
- [23] Zhan, X.; Zhu, D. *Polym. Chem.* **2010**, *1*, 409.
- [24] Boudreault, P. L. T.; Najari, A.; Leclerc, M. *Chem. Mater.* **2011**, *23*, 456.
- [25] Wang, B.; Tsang, S. W.; Zhang, W.; Tao, Y.; Wong, M. S. *Chem. Commun.* **2011**, *47*, 9471.
- [26] Misra, R.; Gautam, P.; Sharma, R.; Mobin, S. M. *Tetrahedron Lett.* **2013**, *54*, 381.
- [27] Zeng, S.; Yin, L.; Jiang, X.; Li, Y.; Li, K. *Dyes Pigm.* **2012**, *95*, 229.
- [28] Wang, J. T.; Ye, H. Y.; Li, H. J.; Mei, C. Y.; Ling, J.; Li, W. S.; Shen, Z. Q. *Chin. J. Chem.* **2013**, *31*, 1367.
- [29] Chen, S. C.; Tang, C. Q.; Yin, Z. G.; Ma, Y. L.; Cai, D. D.; Ganeshan, D.; Zheng, Q. D. *Chin. J. Chem.* **2013**, *31*, 1409.
- [30] Hu, B.; Wang, Y.; Chen, X.; Zhao, Z.; Jiang, Z.; Lu, P.; Wang, Y. *Tetrahedron* **2010**, *66*, 7583.
- [31] Miao, H. M.; Zhang, H. L.; Xu, J. K.; Fan, C. L.; Dong, L.; Zeng, L. Q.; Zhao, F. *Chin. J. Chem.* **2008**, *26*, 1922.
- [32] Zhang, X. C.; Wang, C. Y.; Lai, G. Q.; Zhang, L.; Shen, Y. J. *Polym. Bull.* **2011**, *66*, 893.
- [33] Miyaura, N.; Suzuki, A. *Org. Synth.* **1993**, *8*, 532.
- [34] Lee, P.; Hsu, S. L.; Lee, J. F.; Chuang, H. Y.; Lin, P. J. *Polym. Sci., Part A: Polym. Chem.* **2011**, *49*, 662.
- [35] Li, Y.; Xu, B.; Li, H.; Cheng, W.; Xue, L.; Chen, F.; Lu, H.; Tian, W. *J. Phys. Chem. C* **2011**, *115*, 2386.
- [36] Zhang, T. T.; Zhu, C. Q.; Ma, Y. W.; Wang, C. Y.; Shen, Y. J. *Chin. J.*

- Chem.* **2013**, *31*, 779.
- [37] Hong, D.; Lee, E.; Choi, M. G.; Lee, M. *Chem. Commun.* **2010**, *46*, 4896.
- [38] Sumio, M.; Hirofumi, H.; Tatsuo, W.; Hiroyuki, S. *Synthesis* **2001**, *12*, 1794.
- [39] Hamaguchi, M.; Sawada, H.; Yoshino, K. *Chem. Lett.* **1996**, *18*, 527.
- [40] Lee, K. H.; Lee, H. J.; Morino, K.; Sudo, A.; Endo, T. *Macromol. Chem. Phys.* **2010**, *211*, 2490.
- [41] Lee, K. H.; Lee, H. J.; Morino, K.; Sudo, A.; Endo, T. *J. Polym. Sci., Part A: Polym. Chem.* **2011**, *49*, 1427.
- [42] Dang, T. T. M.; Park, S. J.; Park, J. W.; Chung, D. S.; Park, C. E.; Kim, Y. H.; Kwon, S. K. *J. Polym. Sci., Part A: Polym. Chem.* **2007**, *45*, 5277.
- [43] Leenen, M. A. M.; Meyer, T.; Cucinotta, F.; Thiem, H.; Anselmann, R.; Cola, L. D. *J. Polym. Sci., Part A: Polym. Chem.* **2010**, *48*, 1973.
- [44] Lin, Y.; Li, Y.; Zhan, X. *Chem. Soc. Rev.* **2012**, *41*, 4245.
- [45] Wen, S.; Pei, J.; Zhou, Y.; Li, P.; Xue, L.; Li, Y.; Xu, B.; Tian, W. *Macromolecules* **2009**, *42*, 4977.
- [46] Shirakawa, H.; Louis, E. J.; Macdiarmid, A. G.; Chiang, C. K.; Heeger, A. J. *J. C. S. Chem. Commun.* **1977**, *16*, 578.

(Pan, B.; Qin, X.)